

Zwitterionic Phosphorus Ylide Adducts of Boron-Bridged *ansa*-Zirconocene Complexes as Precatalysts for Olefin Polymerization

Pamela J. Shapiro,^{*[a]} Feilong Jiang,^[a] Xiaoping Jin,^[a] Brendan Twamley,^[a]
Jasson T. Patton,^[b] and Arnold L. Rheingold^[c]

Keywords: Zirconium / Metallocenes / Boron / Ylides / Catalysis

Methylenetriphenylphosphorane was coordinated to the boron of phenylborylidene-bridged bis(cyclopentadienyl)- and bis(2-Me,4-Ph-indenyl)zirconium dichloride to form zwitterionic *ansa*-zirconocene complexes. The cyclopentadienyl complex **2**, when activated with MAO, exhibits remarkable polymerization activity that is more than an order of magnitude greater than that of a related amidoborylidene-bridged complex as well as the commercially important precatalyst [Cp'-SiMe₂-N-*t*Bu]TiCl₂ (Cp' = C₅Me₄). The zwitterionic bis(2-Me,4-Ph-indenyl)zirconium dichloride species is isolated as a mixture of *rac* and *meso* isomers **4–6**. The propylene polymerization efficiency of the isomer mixture

activated by MAO is greater than that of a related silylene bridged system at 70 and 85 °C; however, the activity of the zwitterionic system decreased with further increase in temperature. The high level of isotactic triads (63.6%) and pentads (52.4%) in the polypropylene formed by **4–6** indicates that the *rac* isomer is the most active precatalyst of the mixture. The molecular structures of **2** and the *rac* bis-indenylzirconium isomer **4** and one of the *meso* isomers **5** are described.

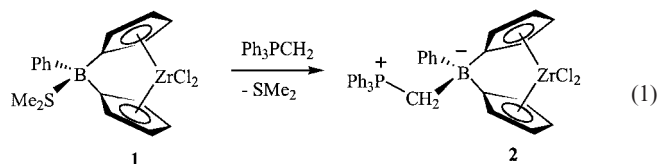
(© Wiley-VCH Verlag GmbH & Co. KGaA, 69451 Weinheim, Germany, 2004)

Introduction

Carbon and silicon are the most common constituents of the bridges connecting the two ancillary ligands in *ansa*-metallocene olefin polymerization catalysts. Bridges based on P,^[1–4] As,^[5] B,^[6–12] and B–P^[13] are also reported. Unique to these heteroatom bridges is the potential to vary their coordination environment and hybridization while the ligand is attached to the metal.

In developing boron-bridged metallocene complexes,^[10–12] one of our objectives is to use the bridging atom as a noncoordinating counteranion for the cationic metal center. Work from our group^[10] and from Bochmann's group^[14] has demonstrated that, in some cases, the boron bridge coordinates anionic moieties such as Cl[−], CH₃[−], and C₆F₅[−] to form stable, isolable salts. The nature of the counteranion and the alkyl anion appear to be crucial in these cases because reactions between complex **1** (Equation 1) and alkylaluminum, Grignard, dialkylzinc, and

alkylaluminum reagents generally lead to decomposition of the complex,^[11] presumably as a result of alkyl anion attack at the boron. When we replaced the weakly bound dimethyl sulfide ligand in **1** with more strongly coordinating trimethylphosphane, we were able to alkylate the zirconium center using alkylaluminum and Grignard reagents.^[15] The trimethylphosphane adduct and the stable borate bridged complexes exhibit ethylene polymerization activity when activated with MAO, but complex **1** does not.^[10]



Since phosphorus ylides have been shown to have a high affinity for Lewis acidic boron centers,^[16–18] we introduced Ph₃PCH₂ onto the boron bridge of the *ansa*-zirconocene complex in order to protect the boron bridge from attack by organometallic alkylating reagents and activators such as MAO. The ylide conferred remarkable ethylene polymerization activity to the complex, prompting us to explore the effectiveness of this adduct in related boron-bridged bis(indenyl)zirconium systems in the context of propylene polymerization catalysis.

^[a] Dept. of Chemistry, University of Idaho, Moscow, ID 83844-2343, USA
Fax: (internat.) +01-208-885-6173
E-mail: shapiro@uidaho.edu

^[b] The Dow Chemical Company, Catalysis Laboratory, Midland, Michigan 48674, USA

^[c] Dept. of Chemistry and Biochemistry, University of California, San Diego, La Jolla, CA 92039-0332, USA

Results and Discussion

Synthesis and Structural Characterization of [(Ph₃CH₂)PhB(η⁵-C₅H₄)₂ZrCl₂]

As shown in Equation 1, Ph₃PCH₂ readily displaces the Me₂S adduct on the boron in **1** to form complex **2**. Single crystals of **2** suitable for an X-ray structure determination were grown from dichloromethane solution. The molecular structure is shown in Figure 1, where pertinent bond lengths and angles are also listed. Crystallographic data is listed in Table 1. The most important geometrical parameters of the molecular structure are the angles about the boron bridge and the tilt of the cyclopentadienyl rings on zirconium. The centroid–Zr–centroid angle (120.2°) and dihedral angle between the cyclopentadienyl rings (66°) are within the range of the other boron-bridged dicyclopentadienylzirconium dichloride complexes.^[10–12] Boron-bridged complexes exhibit greater distortion than silicon-bridged complexes and less distortion than carbon-bridged complexes relative to (η⁵-C₅H₅)₂ZrCl₂.^[12] The Cp–B–Cp angle of 97.1(4)° is close to that of [Me(Ph)BCp₂ZrCl₂][–] [97.2(4)°],^[10] and narrower than that of [Cl(Ph)BCp₂ZrCl₂][–] [99.4(4)°]^[10] and the neutral complexes {(L)PhBCp₂ZrCl₂; L = SMe₂ [101.1(2)°], PMe₃ [100.1(3)°]}.^[11] This indicates that the Lewis basicity of the ylide is similar to that of a methyl anion. The angle about the ylide carbon P(1)–C(17)–B(1) [121.7(3)°] is similar to that of Ph₃CH₂B(C₆F₅)₃ [123.38(10)°].^[18] The P(1)–C(17) [1.788(5) Å] and C(17)–B(1) [1.666(7) Å] bond lengths are

also similar to those of Ph₃CH₂B(C₆F₅)₃ [1.7919(14) Å and 1.675(2) Å, respectively], which has been characterized as a methylene-bridged phosphonium-borate betaine with bond lengths in the range of C(sp³)–X bonds.^[18]

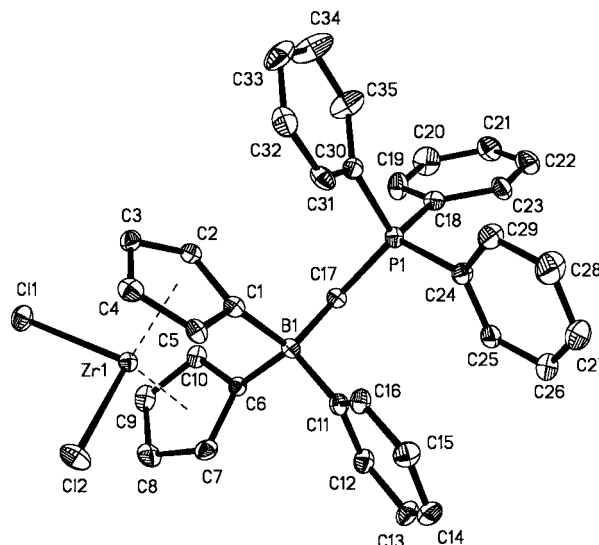


Figure 1. Thermal ellipsoid (30%) drawing of **2**; hydrogen atoms are omitted for clarity; selected bond lengths (Å) and angles (°): B(1)–C(17) 1.666(7), P(1)–C(17) 1.788(5), Zr–cent(1–5) 2.171, Zr–cent(6–10) 2.169, C(1)–B(1)–C(6) 97.1(4), cent–Zr–cent 120.2

Table 1. Crystallographic Data for **2**, **4**, and **5**

	2	4 + 2C ₆ H ₆	5
Formula	C ₃₆ H ₃₁ BCl ₂ PZr	C ₆₉ H ₅₈ BCl ₂ PZr	C ₅₇ H ₄₆ BCl ₂ PZr
Formula mass	773.86	1091.05	934.84
Crystal system	Triclinic	Triclinic	Triclinic
Space group	<i>P</i> $\bar{1}$	<i>P</i> $\bar{1}$	<i>P</i> $\bar{1}$
<i>a</i> (Å)	10.6014(2)	11.8486(7)	13.2315(13)
<i>b</i> (Å)	14.3862	14.6255(9)	13.4195(14)
<i>c</i> (Å)	23.1797(3)	17.1894(11)	16.18550(17)
α (°)	97.2838	81.11(1)	92.515(2)
β (°)	92.0132(7)	72.04(10)	106.197(2)
γ (°)	98.0542(7)	75.36(1)	116.865(2)
<i>V</i> (Å ³)	3467.07(7)	2732.1(3)	2512.9(4)
<i>Z</i>	4	2	2
ρ_{calcd} (Mg/m ³)	1.483	1.326	1.236
μ (mm ^{–1})	0.774	0.371	0.392
<i>F</i> ₀₀₀	1568	1132	964
Crystal size (mm)	0.50 × 0.20 × 0.08	0.15 × 0.14 × 0.04	0.27 × 0.26 × 0.07
θ range (°)	0.89 to 25.00	1.83 to 25.00	1.74 to 25.00?
Index ranges	–12 ≤ <i>h</i> ≤ 14, –19 ≤ <i>k</i> ≤ 18, –30 ≤ <i>l</i> ≤ 30	–14 ≤ <i>h</i> ≤ 14, –17 ≤ <i>k</i> ≤ 17, –20 ≤ <i>l</i> ≤ 20	–15 ≤ <i>h</i> ≤ 15, –15 ≤ <i>k</i> ≤ 15, –20 ≤ <i>l</i> ≤ 20
No. reflections collected	33309	27158	23167
No. independent reflections	15906 [<i>R</i> (int) = 0.0385]	9617 [<i>R</i> (int) = 0.0766]	8810 [<i>R</i> (int) = 0.0603]
Data/restraints/parameters	15906/0/793	9617/0/669	8810/0/561
GOF on <i>F</i> ²	1.187	1.054	1.069
<i>R</i> (<i>F</i> _o) [<i>I</i> > 2σ(<i>I</i>)]	0.0682	0.0682	0.0720
<i>wR</i> (<i>F</i> _o ²) [<i>I</i> > 2σ(<i>I</i>)]	0.2436	0.1319	0.1581
Largest diff. peak/hole e [–] Å ^{–3}	1.694/–1.516	1.038/–0.605	0.949/–1.043

Table 2. Polymerization results for **2** compared with other metallocene systems

Complex	Alkene	Efficiency gP/gM	MW (PDI)
2	ethylene/octene ^[a]	6835920	17200 (2.30)
	propylene ^[b]	27186	ND
[Cp'-SiMe ₂ -N- <i>t</i> Bu]TiCl ₂ (CGC)	ethylene/octene ^[a]	441729	86300 (3.65)
	(<i>i</i> Pr) ₂ N-BCp ₂ ZrCl ₂	346400	8400 (3.93)
Me ₂ SiCp ₂ ZrCl ₂	propylene ^[b]	20984	ND
	ethylene/octene ^[a]	93725	8800 (2.42)
Cp ₂ ZrCl ₂	propylene ^[b]	34421	ND
	ethylene/octene ^[a]	199509	22100 (2.90)
	propylene ^[b]	10962	ND

^[a] 140 °C, 1000 equiv. MAO, 3.4 Mpa ethylene. ^[b] 70 °C, 1000 equiv. MAO, 150 g propylene.

Olefin Polymerization Studies with **2**

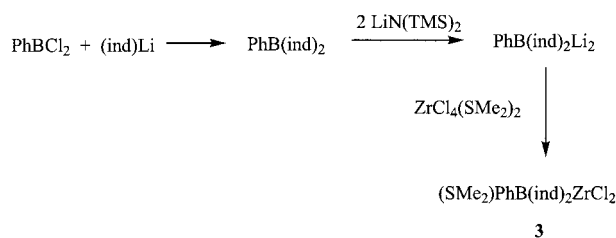
Complex **2** exhibits exceptionally high ethylene polymerization activity when activated with 1000 equiv. of MAO (Table 2). Although the experiment was run in the presence of 1-octene, the high density of the polymer product (>>0.92 g/mL) indicated that little, if any, octene was incorporated. The polymerization efficiency of precatalyst **2** is more than an order of magnitude greater than that of a related amidoborane-bridged system^[6] and the commercially successful precatalyst [Cp'-SiMe₂-N-*t*Bu]TiCl₂^[19] (Cp' = C₅Me₄). Although less impressive, the propylene polymerization efficiency of **2** is comparable with other boron- and silicon-bridged precatalysts.

Bis(indenyl)Zr Analogs of **2**

The favorable performance of **2** as a precatalyst for ethylene and propylene polymerization prompted us to examine boron-bridged bis(indenyl)zirconocene complexes for their propylene polymerization activity. A small number of boron-bridged bis(indenyl)zirconium complexes have been reported.^[6-9] A couple of these exhibit propylene polymerization activities that are comparable with the most active silicon- and carbon-bridged systems.^[6,7] Further, in one case, very high isospecificity from a *rac* isomer was observed.^[7]

To prepare indenyl analogs of **2**, we made some minor modifications to the original synthetic approach to phenylboron-bridged bis(indenyl)zirconium dichloride reported by Reetz et al.^[7] (Scheme 1). With the use of ZrCl₄(SMe₂)₂^[20] as a starting material, we obtained SMe₂ adducts of the boron-bridged complexes instead of ethyl ether adducts. In general, the SMe₂ adducts reacted more cleanly with the phosphane ylides than the ether adducts and afforded higher yields of our target complexes. Initially, we pursued the synthesis of the simple, unsubstituted bis(indenyl) analog of **2**. The poor solubility of this species in toluene and its poor stability in CHCl₃ and CH₂Cl₂ made it difficult to purify. Coordinating solvents such as THF and DMSO were avoided because they competed with the ylide group for coordination to the boron. Furthermore, the ¹H, ¹³C and 2-D NMR spectra of these complexes were of little use for structure identification because of difficulties with sorting indenyl ring resonances from the overlapping

arene resonances of the phenyl rings on the ylide and the boron. We attempted to rectify these problems by replacing Ph₃PCH₂ with Me₃PCH₂. We hoped that Me₃PCH₂ would improve the solubility of the complex, simplify its NMR spectroscopic characterization, and form a more stable adduct with the boron bridge. Unfortunately, the PMe₃CH₂ adduct was even more sensitive to decomposition than the Ph₃PCH₂ adduct, and preliminary screenings of the polymerization activities of the *ansa*-zirconocene complexes indicated that the Ph₃PCH₂ adduct was by far the best candidate.



Scheme 1

The propylene polymerization activity of a sample of the ylide adduct of the boron-bridged bis(indenyl)zirconium complex and the molecular weight of the polymer were promising enough to convince us to modify the indenyl rings in order to form a more soluble system that would be easier to purify. Replacing the indenyl (ind) rings with 2-methyl,4-phenylindenyl^[21] (2-Me,4-Ph-ind) rings gave us a ¹H NMR signal from the 2-Me group that was useful for evaluating the number and ratio of the three *ansa*-zirconocene diastereomers **4-6** (Figure 2) that constituted the product.

The ligand (2-Me,4-Ph-ind)₂BPh was prepared in a manner similar to Reetz's (ind)₂BPh.^[7] In Reetz's synthesis, (ind)₂BPh was treated with the base P(*i*Pr)₃ in order to promote double bond isomerization within the indenyl rings and convert the bridgehead carbon atoms attached to boron from sp³ to sp² so as to reduce the amount of boron-carbon bond cleavage during metallation of the ligand. Since this base-treatment step had no apparent effect on the isomer composition of (2-Me,4-Ph-ind)₂BPh, it was eliminated from our procedure. In addition, harsher conditions were necessary to doubly deprotonate (2-Me,4-Ph-

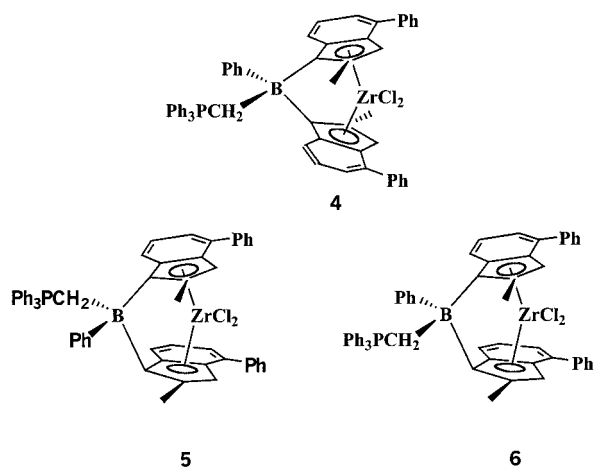


Figure 2. Three diastereomers of $(\text{Ph}_3\text{PCH}_2)\text{B}(2\text{-Me},4\text{-Ph-ind})_2\text{ZrCl}_2$

$\text{ind})_2\text{BPh}$ with $\text{Li}[\text{N}(\text{SiMe}_3)_2]$ (48 h. at 75°C) than were required for $(\text{ind})_2\text{BPh}$. The increased solubility of the *ansa*-zirconocene complexes in hydrocarbon solvents such as benzene and toluene aided in their purification, crystallization, and NMR spectroscopic characterization.

NMR Characterization of Indenyl Complexes 3–6

The presence of two sets of methyl, phenyl, and indenyl resonances in the ^1H NMR spectrum of **3** reveals the presence of two isomers in a 2:1 ratio. Judging from the ratio of diastereomers obtained from the synthesis of **4–6** (vide infra), the predominant species corresponds to the *meso* isomers, and the less abundant isomer is the *rac* species. The appearance of only one set of signals for the *meso* isomers

can probably be attributed to rapid exchange of SMe_2 between the diastereotopic sites on the borylidene bridge.^[11]

A representative ^1H NMR spectrum of a mixture of **4–6**, isolated by crystallization from the bulk reaction product, is shown in Figure 3. With the exception of two olefinic resonances above $\delta = 6$ ppm, the region between 6.5–8.1 ppm containing indenyl and arenyl resonances is quite complex. The methyl and methylene regions (2–4 ppm) of the ^1H spectrum are the most useful for evaluating the isomer composition of the material. A persistent unidentified impurity with ^1H NMR signals upfield of $\delta = 2$ ppm was invariably present in recrystallized samples of the ylide adducts dissolved in CD_2Cl_2 . Since the intensity of the peaks due to this impurity increased over time, and the solvent was predried over molecular sieves, we attribute the impurity to decomposition promoted by the solvent.

The ^{31}P spectrum of the mixture shows three distinct resonances, one for each isomer. The ^{31}P signals were correlated with methylene ^1H NMR resonances by selective phosphorus decoupling (Figure 4). The diastereotopic protons of the methylene group in the *rac* isomer **4** appear as two doublet of doublets (dd) at $\delta = 3.9$ and 3.3 ppm. Saturation of the ^{31}P signal at $\delta = 32.2$ ppm results in their collapse to two doublets. The other ^{31}P resonances at $\delta = 31.8$ and 33.0 ppm must therefore be assigned to the *meso* isomers **5** and **6**. Notably, only one broad ^{11}B resonance at $\delta = -5$ ppm is observed for the isomer mixture. Assignments of the 2-Me peaks of the indenyl rings were based on their intensities relative to the ylide methylene resonances. One of the two inequivalent methyl resonances of **4** is obscured by the methyl resonance of one of the *meso* isomers. We were not successful in purifying the *rac* isomers of either **3** or **4** from their *meso* isomers; however, we did isolate X-ray quality crystals of isomers **4** and **5**, allowing their molecular structures to be determined (vide infra).

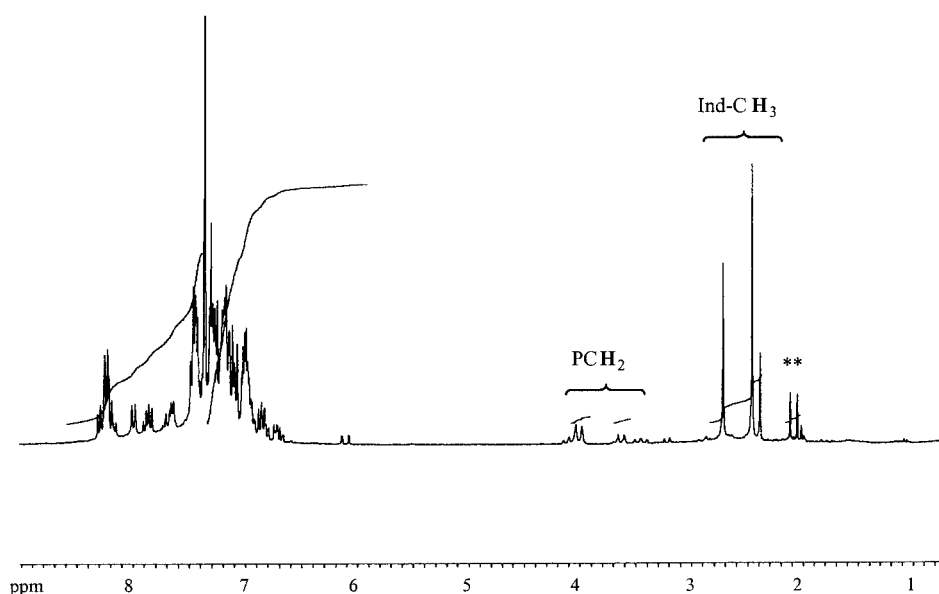


Figure 3. A representative ^1H NMR spectrum of a mixture of **4–6** (* = unidentified impurity); a 3:1 ratio of *meso*:*rac* isomers is observed

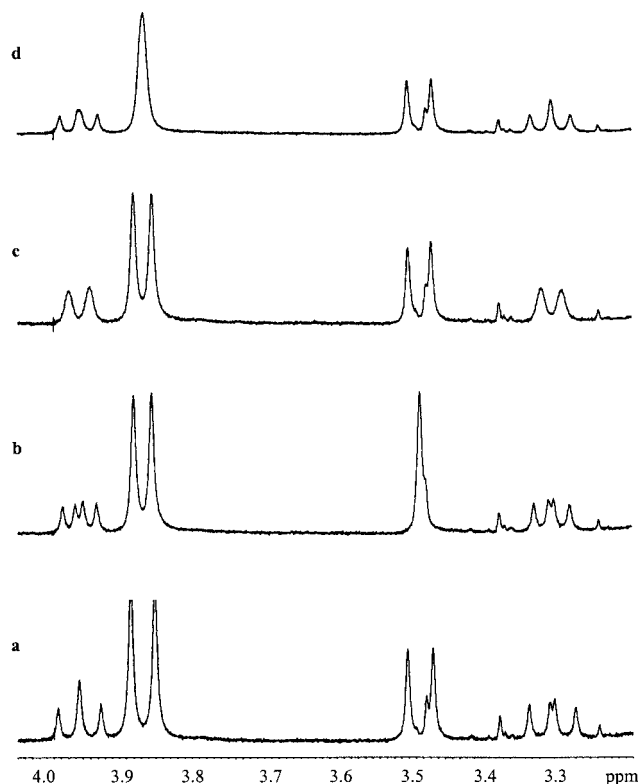


Figure 4. ^1H spectra of ylide CH_2 region of isomer mixture 4–6 with a) no ^{31}P decoupling and selective decoupling of ^{31}P signal at: b) 33.0 ppm, c) $\delta = 32.2$ ppm, d) $\delta = 31.8$ ppm

Crystallographic Characterization of Isomers 4 and 5

The molecular structures of **4** and **5** are shown in Figure 5 and Figure 6, respectively. Crystallographic data for both isomers are included with data for **2** in Table 1. Selected bond lengths and angles for **4** and **5** are listed in Table 3 and Table 4, respectively.

There are three other molecular structures of *rac* boron-bridged bis(indenyl)zirconium complexes in the literature:

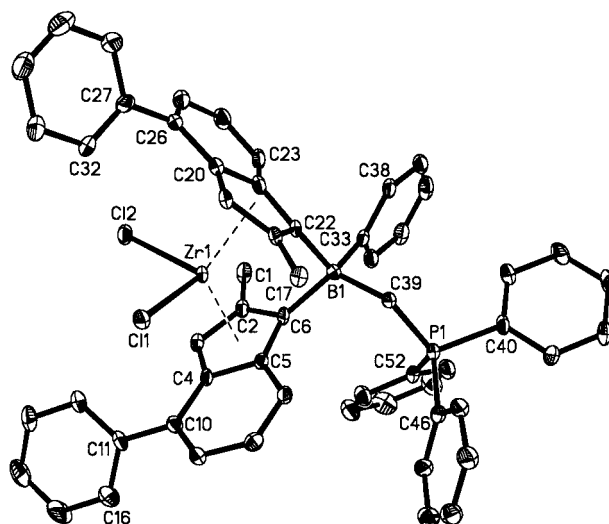


Figure 5. Molecular structure of complex **4**; hydrogen atoms are omitted for clarity

(*L*)PhB(ind) $_2$ ZrCl $_2$ (*L* = THF, PMe $_3$) published by Reetz,^[7] and the structure of *iPr* $_2$ NB(ind)ZrCl $_2$ published by Ashe.^[6] Of the four structures, **4** has the smallest angle between the boron and the indenyl bridgehead carbon atoms; 97.6(3) $^\circ$ for **4** vs. 101.5 (*L*=THF) and 99.4 (*L*=PMe $_3$) for (*L*)PhB(Ind) $_2$ ZrCl $_2$, and 104.9 $^\circ$ for *iPr* $_2$ NB(ind) $_2$ ZrCl $_2$. Nevertheless, the centroid–Zr–centroid angle for **4** (123.2 $^\circ$) is slightly larger than those of (*L*)PhB(Ind) $_2$ ZrCl $_2$ (122.3, *L*=THF; 121.5, *L*=PMe $_3$), and the dihedral angle between the indenyl ring planes of **4** (65.7 $^\circ$) is slightly smaller than that of *iPr* $_2$ NB(Ind) $_2$ ZrCl $_2$ (66.8 $^\circ$). Thus, small changes in the bite angle at boron has little effect on the geometry between the indenyl rings on the zirconium. On the other hand, changing the size of the bridging atom does influence the geometry of the metallocene, with silicon affording a more relaxed structure with a dihedral angle of 62 $^\circ$ between the rings and carbon causing a more open structure with an angle of 71 $^\circ$ between the ring planes.^[12]

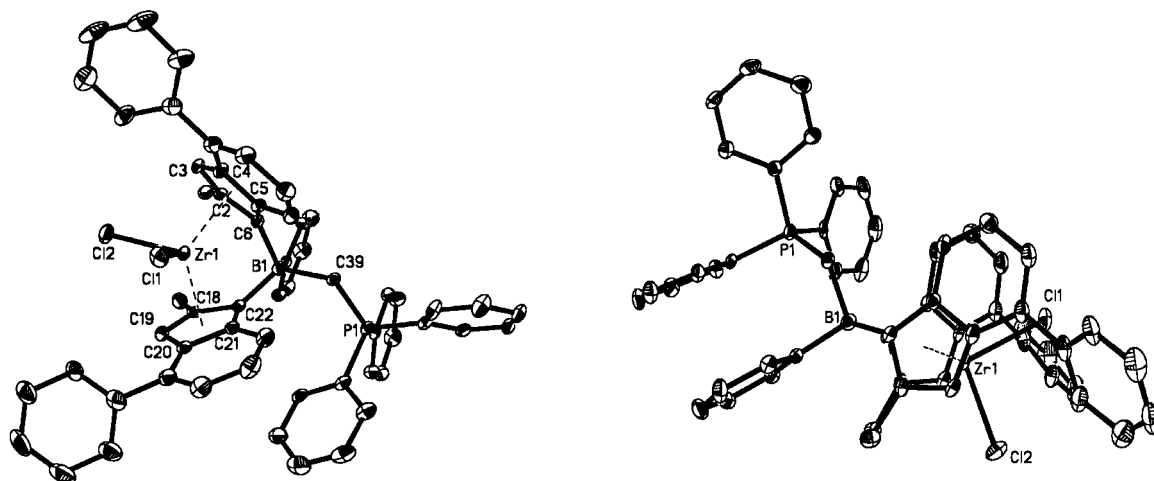


Figure 6. Thermal ellipsoid (30%) drawing of **5** [side (a) and top (b) views]; hydrogen atoms are omitted for clarity

Table 3. Selected bond lengths (Å) and angles (°) for **4**

Zr(1)–Cl(2)	2.4285(13)	C(5)–C(6)	1.454(6)
Zr(1)–Cl(1)	2.4491(12)	C(18)–C(19)	1.395(6)
B(1)–C(33)	1.630(7)	C(18)–C(22)	1.431(6)
B(1)–C(39)	1.662(7)	C(2)–C(3)	1.404(6)
B(1)–C(6)	1.667(7)	C(2)–C(6)	1.434(6)
B(1)–C(22)	1.679(7)	C(19)–C(20)	1.398(6)
P(1)–C(39)	1.807(5)	C(20)–C(21)	1.433(7)
Zr(1)–C(22)	2.440(4)	C(21)–C(22)	1.460(6)
Zr(1)–C(6)	2.449(4)	C(21)–C(23)	1.419(7)
Zr(1)–C(18)	2.482(4)		
Zr(1)–C(2)	2.489(5)	C(33)–B(1)–C(39)	102.1(4)
Zr(1)–C(5)	2.501(4)	C(33)–B(1)–C(6)	118.7(4)
Zr(1)–C(21)	2.508(4)	C(39)–B(1)–C(6)	115.5(4)
Zr(1)–C(19)	2.546(5)	C(33)–B(1)–C(22)	111.9(4)
Zr(1)–C(3)	2.549(5)	C(39)–B(1)–C(22)	111.3(4)
Zr(1)–C(4)	2.590(4)	C(6)–B(1)–C(22)	97.6(3)
Zr(1)–C(20)	2.597(5)	Cl(2)–Zr(1)–Cl(1)	96.96(4)
cent(2–6)–Zr	2.203	B(1)–C(39)–P(1)	123.2(4)
cent(18–22)–Zr	2.205	cent–Zr–cent	123.2
C(3)–C(4)	1.407(6)	ind/ind	65.7
C(4)–C(5)	1.452(6)		

Table 4. Selected bond lengths (Å) and angles (°) for **5**

Zr(1)–Cl(1)	2.4038(14)	C(3)–C(4)	1.401(7)
Zr(1)–Cl(2)	2.4547(14)	C(4)–C(5)	1.441(6)
B(1)–C(33)	1.623(7)	C(5)–C(6)	1.447(7)
B(1)–C(22)	1.660(8)	C(18)–C(19)	1.390(7)
B(1)–C(6)	1.660(7)	C(18)–C(22)	1.457(7)
B(1)–C(39)	1.695(7)	C(19)–C(20)	1.401(7)
P(1)–C(39)	1.793(4)	C(20)–C(21)	1.433(7)
Zr(1)–C(2)	2.499(5)	C(21)–C(22)	1.461(7)
Zr(1)–C(3)	2.559(5)		
Zr(1)–C(5)	2.502(5)	C(6)–B(1)–C(39)	110.3(4)
Zr(1)–C(6)	2.445(4)	C(33)–B(1)–C(39)	104.0(4)
Zr(1)–C(4)	2.604(5)	C(33)–B(1)–C(6)	113.4(4)
Zr(1)–C(18)	2.491(5)	C(33)–B(1)–C(22)	116.2(4)
Zr(1)–C(19)	2.546(5)	C(22)–B(1)–C(6)	98.2(4)
Zr(1)–C(20)	2.626(5)	C(22)–B(1)–C(39)	115.1(4)
Zr(1)–C(21)	2.482(5)	B(1)–C(39)–P(1)	125.7(3)
Zr(1)–C(22)	2.455(4)	Cl(1)–Zr–Cl(2)	97.49(5)
C(1)–C(2)	1.501(7)	cent–Zr–cent	123.2
C(2)–C(3)	1.411(6)	ind/ind	68.3
C(2)–C(6)	1.445(6)		

The geometric features of the boron-ylide adduct in **4** are very similar to those of **2**, even though chemically, the interaction appears to be weaker in **4**. The bond lengths B(1)–C(39) [1.662(7) Å] and P(1)–C(39) [1.807(5) Å] are very similar to the corresponding distances in **2**, as is the bond angle B(1)–C(39)–P(1) [123.2(4)°].

The molecular structure of **5** is the first structure of a *meso* isomer of a borylidene-bridged bis(indenyl)zirconium complex and is one of very few reported structures of *meso* *ansa*-bis(indenyl)zirconocene complexes of any kind reported in the literature.^[22,23] The noticeable influence of the span of the bridge on the tilt of the indenyl rings is evident by comparing the cent–Zr–cent angle and of **5** (123.2°) and the dihedral angle between the ring planes (68.3°) with the corresponding angles of ethandiyl-bridged *meso*-C₂H₄[4,4'-(2,7-dimethylindenyl)₂]ZrCl₂ (131.8° and 52.9°, respec-

tively).^[22] The bond lengths and angles of the boron-ylide portion of the structure are, within statistical error, similar to the values for **2** and **4**.

Polymerization Activity of (Ph₃pch₂)PhB(2-Me,4-Ph-Ind)₂ZrCl₂ (**4–6**) as a Mixture of Isomers

The propylene polymerization activity of the mixture of *meso* and *rac* diastereomers **4–6** activated with MAO is compared with that of the silicon-bridged complex *rac*-SiMe₂(2-Me,4-Ph-Ind)₂Zr(1,4-Ph₂-butadiene)^[24,25] (**7**) in Table 5. The activity of the mixture of boron-bridged species is more than twice that of the silicon-bridged complex at 70 °C and 85 °C; however, the activity of **4–5** drops substantially at ≥100 °C, while the activity of **7** increases at higher temperatures. The molecular weight of the polymer product starts out higher for **4–6** than for **7** and drops with increasing temperature for both systems. The polydispersity indexes are close to 2 for both systems, at least at the lower temperatures of 70 °C and 85 °C, signifying the homogeneity of the active catalyst centers. The narrow polydispersity and relatively high melting temperature of the polymer produced by **4–6** suggests that the *rac* isomer **4** is the most active species in the mixture of isomers. Indeed, ¹³C NMR analysis of the microstructure of the polypropylene product formed by **4–6** reveals a 63.6:26.5:9.8 ratio of mm:mr:rr triads and a mmmm pentad composition of 52.4%.

Table 5. Propylene polymerization results for isomer mixture **4–6** and **7**

Complex	T _p (°C)	Efficiency gP/gZr	MW (PDI)	T _m (°C)
4–6	70	1081024	373000 (1.96)	156.2
4–6	85	1020311	196000 (2.24)	155.3
4–6	100	713375	132000 (2.14)	154.5
4–6	115	333920	31900 (2.89)	152.7
7	70	450108	513000 (1.80)	158.8
7	85	502987	309000 (2.00)	156.8
7	100	834442	184400 (3.30)	153.7
7	115	900218	79800 (2.81)	153.7

Conclusion

The exceptionally high ethylene polymerization activity of MAO-activated **2** is a result that we do not yet understand. We are currently preparing alkyl derivatives of this system in order to examine their reactivity with various Lewis-acid activators to elucidate the nature of the active catalyst.^[26]

Complex **2** is considerably more stable than its indenyl analogs **4–6**. Whereas **2** is stable indefinitely in chloroform or dichloromethane solution, the indenyl complexes decompose in these solvents. In addition, the indenyl compounds decompose over weeks in the solid state if they are not refrigerated (–30 °C).

Although at 70 °C and 85 °C the performance of **4–6** as precatalysts for propylene polymerization was significantly

better than that of a silicon-bridged species used as a benchmark in industry, the poor thermal stability of the boron-bridged system and our inability to isolate the *rac* isomer **4** from the mixture diminishes its utility.

The fairly high percentage of isotactic triads (63.6%) and pentads (52.4%) in the polypropylene formed with **4–6** is interesting because it indicates that *rac* isomer **4** is the most active species among the three diastereomers, since it constitutes only about 25% of the mixture. A more dramatic effect of the higher activity of a *rac* isomer on the isotacticity of polypropylene produced by a mixture of *rac* and *meso ansa*-zirconocene species has been reported by Collins et al.^[22]

Alternative synthetic methods designed to increase selectivity for *rac* isomer **4** were explored, such as the reaction between (Ph)B(2-CH₃-4-Ph-ind)₂ and Zr(NMe₂)₄^[27,28] and the reaction of (Ph)B(2-CH₃-4-Ph-ind)₂Li₂ with either Cl₂(PEt₃)₂Zr(η²-1,4-Ph₂-C₄H₄)^[24,25] or Cl₂(THF)Zr[PhN(CH₂)₃NPh]^[29] these methods have been used successfully for the *rac*-selective synthesis of other bridged bis(indenyl)-zirconium complexes. Unfortunately, these approaches did not afford isolable *ansa*-zirconocene products.

The preparation of other ylde-like adducts of these boron-bridged *ansa*-zirconocene complexes is currently being explored in order to generate more stable species from which the pure *rac* isomer can be isolated.

Experimental Section

General Remarks: All manipulations were carried out under argon atmosphere using Schlenk and glovebox techniques. Argon and nitrogen were purified by passage over an oxy tower BASF catalyst (Aldrich) and molecular sieves (4 Å). ¹H, ¹³C, ¹¹B, and ³¹P NMR spectra were recorded on Varian Unit Plus 400 MHz NMR (100 MHz ¹³C) IBM NR-300 (300 MHz ¹H; 75 MHz ¹³C) and Bruker AVANCE 500 spectrometers (500 MHz ¹H; 125 MHz ¹³C). ¹H and ¹³C spectra were referenced to residual protons in the solvent. ¹¹B and ³¹P were referenced to external standards (BF₃·OEt₂ and 80% H₃PO₄). Deuterated solvents were dried over molecular sieves (4 Å). PhBCl₂ (Aldrich) was used as received. Toluene, benzene, pentane, petroleum ether, and dichloromethane solvents were dried over alumina and stored in line pots over Na/benzophenone or CaH₂ in the case of dichloromethane. Me₂S(Ph)B(η⁵-C₅H₄)₂ZrCl₂^[11] and Ph₃PCH₂^[30] were prepared according to literature procedures. 2-Methyl-4-phenylindene was prepared as described in the literature^[21] and was also purchased from Boulder Scientific and used as received. Elemental analyses were performed by Desert Analytics (Tucson, Az).

Ph₃PCH₂(Ph)B(η⁵-C₅H₄)₂ZrCl₂ (2**):** Toluene (80 mL) was transferred to a mixture of Ph₃PCH₂ (1.71 g, 6.2 mmol) and **1** (3.30 g, 6.2 mmol) in a flask cooled to -78 °C. The reaction solution was warmed to room temperature and stirred for 18 h to give a grey suspension. The precipitate was isolated by filtration and washed with toluene (30 mL × 2), and dried under vacuum. The resulting yellow-grey solid was redissolved in dichloromethane (20 mL) and layered with pentane. Slow diffusion of the pentane into the dichloromethane caused the precipitation of crystalline product, which was washed with pentane (30 mL × 2) and dried under vac-

uum (yield: 3.05 g, 75%). ¹H NMR (300 K, CDCl₃): δ = 7.57 (m, 3 H, C₆H₅), 7.38 (m, 14 H, C₆H₅), 6.97 (m, 3 H, C₆H₅), 6.60 (m, 4 H, C₅H₄), 5.51 (m, 4 H, C₅H₄), 2.67 (d, ²J_{PH} = 16.5 Hz, 2 H, PCH₂) ppm. ¹³C{¹H} NMR (300 K, CDCl₃): δ = 135, 133.3 (BC₆H₅), 133.4, 133.3, 129.2, 129.1 (PC₆H₅), 127.112, 125.0, 124.8 (C₅H₄), 122.9 (d, ¹J_{P,C} = 84 Hz, PCH₂) ppm. ³¹P{¹H} NMR (300 K, CDCl₃): δ = 37.1 ppm. ¹¹B NMR (300 K, CDCl₃): δ = -9.1 ppm. C₃₅H₃₀BCl₂PZr (654.5): calcd. C 64.22, H 4.62; found C 64.03, H 4.71.

(Ph)(2-CH₃-4-Ph-ind)₂B: PhBCl₂ (1.3 mL, 1.58 g, 10 mmol) was added to a solution of (2-Me,4-Ph-ind)Li (4.2 g, 20 mmol) in Et₂O (70 mL) at -78 °C. The reaction mixture turned from red to yellow as it warmed to room temperature. After stirring for 15 h, the reaction was filtered, and the filtrate was dried under vacuum, to give a yellow solid that consisted of (Ph)(2-CH₃-4-Ph-ind)₂B as a mixture of double bond isomers complexed by 0.5 equiv. Et₂O (yield: 4.8 g, 91%). ¹H NMR (300 K, C₆D₆): δ = 7.60–7.50 (m, 6 H, C₆H₅), 7.30–7.01 (m, 30 H, C₆H₅ + PhC₆H₃), 6.50 (d, PhC₆H₃), 4.18, 4.11 (s, 2 H, MeC₅H₂), 3.01 (m, 2 H, Et₂O), 1.84, 1.81, 1.73 (s, 6 H, CH₃), 0.90 (3 H, Et₂O) ppm.

(Ph)B(2-CH₃-4-Ph-Ind)₂Li₂: Lithium bis(trimethylsilyl)amide (2.88 g, 17.20 mmol) was added to a solution of (Ph)B(2-CH₃-4-Ph-ind)₂ (4.20 g, 7.93 mmol) in toluene (150 mL) cooled to -78 °C. The reaction mixture was allowed to warm to room temperature and then heated at 75 °C with stirring for 48 h to give a suspension. The precipitate was isolated by filtration and washed with toluene (30 mL × 2) and petroleum ether (50 mL), and dried under vacuum, to give a grey-orange solid (yield: 2.30 g, 54%). ¹H NMR (300 K, [D₆]DMSO): δ = 7.73 (d, ³J_{H,H} = 7.4 Hz, 6 H, C₆H₅), 7.34 (t, ³J_{H,H} = 7.5 Hz, 9 H, C₆H₅), 7.13 (t, ³J_{H,H} = 7.0 Hz, 2 H, indenyl), 6.78 (d, ³J_{H,H} = 7.8 Hz, 2 H, 6.29 (m, 2 H, indenyl), 6.06 (m, 2 H, indenyl), 1.89 (s, 6 H, CH₃) ppm.

Me₂S(Ph)B(2-CH₃-4-Ph-ind)₂ZrCl₂ (3**):** Zr(SMe₂)₂Cl₄ solid (0.98 g, 2.74 mmol) was added to a suspension of (Ph)B(2-CH₃-4-Ph-ind)₂Li₂ (1.40 g, 2.74 mmol) in toluene (120 mL) cooled to -78 °C. The mixture was allowed to warm to room temperature and stirred for 18 h. After filtration to remove LiCl, the volatiles were removed from the filtrate under vacuum. The filtrate residue was washed with petroleum ether (30 mL × 2) and dried under vacuum (yield: 1.70 g, 86%). Recrystallization of **3** from benzene/pentane gave a red-brown, crystalline product with the formula **3**·4C₆H₆. ¹H NMR (300 K, C₆D₆): minor isomer (*rac*): δ = 7.91 (d, ³J_{H,H} = 7.2 Hz, 6 H, C₆H₅) 6.46, 6.77 (m, 6 H, C₆H₅), 2.11 (s, 6 H, CH₃) ppm; major isomer (*meso*): δ = 7.90 (d, ³J_{H,H} = 7.2 Hz, 6 H, C₆H₅), 6.61 (m, 6 H, C₆H₅), 2.09 (s, 6 H, CH₃) ppm; both isomers: δ = 7.55–7.0 (m, 22 H, indenyl and C₆H₅), 2.24 (s, 12 H, SCH₃) ppm. ¹³C{¹H} NMR (300 K, C₆D₆): δ 140.23, 139.97, 138.82, 137.54, 137.51, 134.30, 133.64, 131.19, 129.81, 128.84, 128.81, 128.76, 128.65, 128.62, 128.58, 128.55, 128.23, 125.49, 125.17, 123.41, 119.06, 117.86, 108.11, 106.89, 104.88, 19.30, 12.29, 19.14, 17.33, 16.45, 16.36. No ¹¹B signal was detected, possibly due to extreme broadening caused by rapid exchange of the Me₂S adduct. C₄₆H₄₁ZrCl₂B (766.8): calcd. C 74.69, H 5.39; found C 74.67, H 5.13.

Ph₃PCH₂(Ph)B(2-CH₃-4-Ph-Ind)₂ZrCl₂ (4–6**):** Ph₃PCH₂ (511 mg, 1.85 mmol) was added to a solution of **3** (1.21 g, 1.85 mmol) in toluene (120 mL) at -78 °C, and the reaction was warmed to room temperature with stirring. The reaction solution was dark red in color after it was stirred at room temperature for 18 h. After filtration, the volatiles were removed from the filtrate under reduced pressure, and the residue was washed with pentane (50 mL × 2) and dried under vacuum to give a red solid. Recrystallization of the

red solid from a benzene solution over which pentane was layered afforded red crystals that were suitable for X-ray diffraction studies. The crystals were washed with pentane and dried under vacuum (yield: 795 mg, 46%). ^1H NMR (300 K, C_6D_6): all isomers: δ 8.2–8.0 (m, C_6H_5), 7.88 (d, C_6H_5), 7.71 (m, C_6H_5), 7.59 (d, C_6H_5), 7.4–6.5 (large m) ppm; **4**: 3.96 (dd, $^2J_{\text{PH}} = 17.5$, $^2J_{\text{H,H}} = 15$ Hz, 1 H, PCH_2), 2.25 (s, 3 H, CH_3), 2.18 (s, 3 H, CH_3) ppm; **5** and **6**: 3.87 (d, $^2J_{\text{PH}} = 16.6$ Hz, 1 H, PCH_2), 3.49 (d, $^2J_{\text{PH}} = 16.5$ Hz, 1 H, PCH_2), 3.30 (dd, $^2J_{\text{PH}} = 17.5$, $^2J_{\text{H,H}} = 15$ Hz, 1 H, PCH_2), 2.52 (s, 3 H, CH_3), 2.26 (s, 3 H, CH_3) ppm. ^{13}C NMR (300 K, C_6D_6): $\delta = 141.42, 136.48, 133.81, 130.65, 130.04, 129.19, 129.10, 129.19, 128.95, 128.72, 128.45, 128.34, 128.10, 126.98, 125.62, 124.48, 124.44, 123.78, 122.88, 122.06, 121.62, 118.87, 118.48, 108.37, 107.09, 104.89, 102.89, 42.75, 42.64, 21.51, 21.22, 21.04, 20.91$ ppm. ^{31}P NMR (300 K, C_6D_6): **4**: $\delta = 32.21$ ppm; **5** and **6**: $\delta = 31.8, 33.0$ ppm. ^{11}B NMR (300 K, C_6D_6): $\delta = -5$ ppm. $\text{C}_{57}\text{H}_{46}\text{BCl}_2\text{PZr}$ (934.9): calcd. C 73.23, H 4.96; found C 68.30, H 4.85. Carbon was repeatedly low when reanalyzed. We attribute this to impurities that we were unable to remove from the sample.

Ethylene/Octene Copolymerizations: All feeds were passed through columns of activated alumina and Q-5TM catalyst prior to introduction to the reactor. A stirred 2-L Parr reactor was charged with Isopar-E solvent (about 740 g) and 1-octene comonomer (118 g). Hydrogen was added as a molecular weight control agent by differential pressure expansion from a 75 mL addition tank at 25 psi (2070 kPa). The reactor contents were then heated to the polymerization temperature of 140 °C and saturated with ethylene at 500 psig (3.4 Mpa). The metal complex and activators were mixed as dilute toluene solutions, transferred to a catalyst addition tank and injected into the reactor through a stainless steel transfer line. The polymerization conditions were maintained for 15 minutes with ethylene added on demand to keep the pressure constant. Heat was continually removed from the reaction with an internal cooling coil. The resulting solution was removed from the reactor, quenched with isopropyl alcohol, and stabilized by the addition of a toluene solution (10 mL) containing a hindered phenol antioxidant (approximately 67 mg, IrganoxTM 1010 from Ciba Geigy Corporation) and a phosphorus stabilizer (approximately 133 mg, IrgafosTM 168 from Ciba Geigy Corporation). Between polymerization runs, a wash cycle was conducted in which mixed alkanes were added (850 g) to the reactor that was then heated to 150 °C. The reactor was then emptied of the heated solvent immediately prior to a new polymerization run.

Propylene Polymerizations: All feeds were passed through columns of activated alumina and Q-5TM catalyst prior to introduction to the reactor. A stirred 2-L jacketed Autoclave Engineers Zipper-ClaveTM reactor was charged with Isopar-E solvent (about 625 g) and propylene (about 150 g). Hydrogen was added as a molecular weight control agent by differential pressure expansion from a 75 mL addition tank ($\Delta 350$ kPa). The reactor was heated to 70 °C and allowed to equilibrate. The metal complex and activators were mixed as dilute toluene solutions, transferred to a catalyst addition tank and injected into the reactor through a stainless steel transfer line. Heat was continually removed from the reaction with a cooling coil in the jacket. The resulting mixture was removed from the reactor.

Polymers were recovered by drying for about 20 h in a vacuum oven set at 140 °C. High temperature gel permeation chromatography (GPC) analysis of polymer samples were carried out in 1,2,4-trichlorobenzene at 135 °C on a Waters 150C high temperature instrument. A polystyrene/polyethylene or polypropylene universal calibration was carried out on the isolated polyethylene or polypro-

pylene polymer samples using narrow molecular weight distribution polystyrene standards from Polymer Laboratories.

$^{13}\text{C}\{^1\text{H}\}$ NMR Analysis of Polypropylene: The solution ^{13}C analysis was performed on a Varian Unit Plus 400 MHz NMR spectrometer. The sample was prepared by heating the polymer (0.4 g) to 150 °C in a mixture of $[\text{D}_2]$ tetrachloroethane/orthodichlorobenzene (3.0 g of 50:50 wt. mixture) containing 0.025 M chromium acetylacetonate until homogenized. The data were acquired at 120 °C using continuous ^1H decoupling, 4000 transients per data file, and a 0.7 s pulse repetition delay.

X-ray Crystallographic Study: Yellow crystals of **2** obtained by recrystallization from chloroform were sealed in capillaries under N_2 . A suitable crystal was selected, and data were collected at 173 K on a Siemens P4/CCD instrument (Mo- $K\alpha$ radiation, $\lambda = 0.71073$ Å). Crystals of **4** and **5** obtained by recrystallization from benzene/petroleum ether were covered with a layer of hydrocarbon oil. Suitable crystals of each were selected, attached to glass fibers, and placed in a low-temperature nitrogen stream. Data for both **4** and **5** were collected at 203(2) K on a Bruker/Siemens SMART APEX instrument (Mo- $K\alpha$ radiation, $\lambda = 0.71073$ Å) equipped with a Siemens LT-2A low temperature device. Data were measured using omega scans of 0.3° per frame for 10 s, and a half sphere of data was collected. A total of 1471 frames were collected for each crystal with a final resolution of 0.84 Å. The first 50 frames were recollected at the end of data collection to monitor for decay. Cell parameters were retrieved with SMART software and refined with SAINTPlus on all observed reflections (SMART: v. 5.625 and SAINTPlus: v. 6.22, Bruker AXS, Madison, WI). Data reduction and correction for Lorentz polarization and decay were performed using the SAINTPlus software. Absorption corrections were applied to **2**, **4** and **5** with SADABS (SADABS: v. 2.01, Sheldrick, G.M., Bruker AXS Inc., Madison, WI).

All three structures were solved by direct methods and all refined by the least-squares method on F^2 with the SHELXTL program package (SHELXTL v. 5.10, Bruker AXS Inc., Madison, WI). All three structures were solved in the space group $P\bar{1}$ (# 2) by analysis of systematic absences. Non-hydrogen atoms were refined anisotropically. Hydrogen atoms were added geometrically and refined with a riding model with their parameters constrained to the parent atom site.

The structure of **2** contains two crystallographically independent molecules along with two molecules of chloroform in the asymmetric unit. The structure of **5** contains large voids in the asymmetric unit (ca. 446 Å³). An irresolvable mixture of the solvent of crystallization, petroleum ether, occupied these voids. The solvent contribution to the scattering was removed using the SQUEEZE routine in PLATON,^[31] and approximately 76 electrons were removed. No decomposition was observed during the collection for any of the crystals.

CCDC-226719 to -226721 contains the supplementary crystallographic data for this paper. These data can be obtained free of charge at www.ccdc.cam.ac.uk/conts/retrieving.html [or from the Cambridge Crystallographic Data Centre, 12 Union Road, Cambridge CB2 1EZ, UK; Fax: +44 1223/336-033; E-mail: deposit@ccdc.cam.ac.uk].

Acknowledgments

Financial support for this work was provided by The Dow Chemical Company. P. J. S. thanks the referees for this manuscript for their helpful suggestions.

- [1] H. Köpf, N. Klouras, *Monatsh. Chem.* **1983**, *114*, 243–247.
- [2] J. H. Shin, T. Hascall, G. Parkin, *Organometallics* **1999**, *18*, 6–9.
- [3] J. H. Shin, B. M. Bridgewater, G. Parkin, *Organometallics* **2000**, *19*, 5155–5159.
- [4] N. Leyser, K. Schmidt, H.-H. Brintzinger, *Organometallics* **1998**, *17*, 2155–2161.
- [5] N. Klouras, *Z. Naturforsch., Teil B* **1991**, *46*, 647–649.
- [6] A. J. Ashe, X. Fang, J. W. Kampf, *Organometallics* **1999**, *18*, 2288–2290.
- [7] M. T. Reetz, M. Willuhn, C. Psiorz, R. Goddard, *Chem. Commun.* **1999**, 1105–1106.
- [8] K. A. Ruffanov, V. V. Kotov, N. B. Kazennova, D. A. Lemenovskii, E. V. Avtomonov, J. Lorberth, *J. Organomet. Chem.* **1996**, *525*, 287–289.
- [9] K. Ruffanov, E. Avtomonov, N. Kazennova, V. Kotov, A. Khvorost, D. Lemenovskii, J. Lorberth, *J. Organomet. Chem.* **1997**, *536–537*, 361–373.
- [10] C. T. Burns, D. S. Stelck, P. J. Shapiro, A. Vij, *Organometallics* **1999**, *18*, 5432–5434.
- [11] D. S. Stelck, P. J. Shapiro, N. Basicckes, *Organometallics* **1997**, *16*, 4546–4550.
- [12] P. J. Shapiro, *Eur. J. Inorg. Chem.* **2001**, 321–326.
- [13] K. Aleksander, O. Starzewski, W. M. Kelly, A. Stumpf, D. Freitag, *Angew. Chem. Int. Ed.* **1999**, *38*, 2439–2442.
- [14] S. J. Lancaster, M. Bochmann, *Organometallics* **2001**, *20*, 2093–2101.
- [15] D. S. Stelck, PhD Thesis, University of Idaho, **2001**.
- [16] H. Schmidbaur, G. Mueller, G. Blaschke, *Chem. Ber.* **1980**, *113*, 1480–6.
- [17] H. J. Bestmann, K. Suehs, T. Roeder, *Angew. Chem.* **1981**, *93*, 1098–1100.
- [18] S. Doering, G. Erker, R. Froehlich, O. Meyer, K. Bergander, *Organometallics* **1998**, *17*, 2183–2187.
- [19] A. L. McNight, R. M. Waymouth, *Chem. Rev.* **1998**, *98*, 2587–2598, and references cited therein.
- [20] E. C. Lund, T. Livinghouse, *Organometallics* **1990**, *9*, 2426–2427.
- [21] W. Spaleck, F. Küber, A. Winter, J. Rohrmann, B. Bachmann, M. Antberg, V. Dolle, E. Paulus, *Organometallics* **1994**, *13*, 954–963.
- [22] S. Collins, W. J. Gauthier, D. A. Holden, B. A. Kuntz, N. J. Taylor, D. G. Ward, *Organometallics* **1991**, *10*, 2061–2068.
- [23] T. Kato, H. Uchin, N. Iwama, K. Imaeda, M. Kashimoto, in *Metalorganic Catalysts for Synthesis and Polymerization* (Ed.: W. Kaminsky), Springer-Verlag, Berlin, **1999**, pp. 195.
- [24] E. Y. Chen, D. D. Devore, R. E. Campbell, D. P. Green, J. T. Patton, J. Soto, D. R. Wilson, US Patent 6,127,563, (Dow Chemical Co.), **2000**.
- [25] F. J. Timmers, J. C. Stevens, D. D. Devore, R. K. Rosen, J. T. Patton, D. R. Neithamer, US Patent 6,465,384 B1, (Dow Chemical Co.), **2002**.
- [26] Note added in proof: Per the suggestion of a referee, we examined an NMR scale reaction between **2** and two molar equivalents of AlMe₃ in C₆D₆ in order to determine if MAO is possibly destructive to the complex. One major new species was observed, which we tentatively assign as the dimethylzirconium analog of **2**, along with two minor zirconocene species. Some decomposition was also apparent. There is no evidence of methane production, nor is there any evidence of ylide abstraction from the zirconocene by AlMe₃. We verified this by comparing the ³¹P and ¹H NMR spectroscopic data for the reaction with that of a direct reaction between the ylide and AlMe₃.
- [27] G. M. Diamond, S. Rodewald, R. F. Jordan, *Organometallics* **1995**, *14*, 5–7.
- [28] G. M. Diamond, R. F. Jordan, J. L. Petersen, *J. Am. Chem. Soc.* **1996**, *118*, 8024–8033.
- [29] X. Zhang, Q. Zhu, I. A. Guzei, R. F. Jordan, *J. Am. Chem. Soc.* **2000**, *122*, 8093–8094.
- [30] H. Schmidbaur, H. Stuhler, W. Vornberger, *Chem. Ber.* **1972**, *105*, 1084–1086.
- [31] A. L. Spek, *Acta Crystallogr., Sect. A* **1990**, *46*, C-34.

Received December 14, 2003
Early View Article
Published Online June 7, 2004